nature chemistry

ARTICLES

PUBLISHED ONLINE: 29 JULY 2012 | DOI: 10.1038/NCHEM.1411

In situ surface coverage analysis of RuO_2-catalysed HCl oxidation reveals the entropic origin of compensation in heterogeneous catalysis

Detre Teschner[1,2]*, Gerard Novell-Leruth[3], Ramzi Farra[1], Axel Knop-Gericke[1], Robert Schlögl[1], László Szentmiklósi[2], Miguel González Hevia[3], Hary Soerijanto[4], Reinhard Schomäcker[4], Javier Pérez-Ramírez[5] and Núria López[3]*

In heterogeneous catalysis, rates with Arrhenius-like temperature dependence are ubiquitous. Compensation phenomena, which arise from the linear correlation between the apparent activation energy and the logarithm of the apparent pre-exponential factor, are also common. Here, we study the origin of compensation and find a similar dependence on the rate-limiting surface coverage term for each Arrhenius parameter. This result is derived from an experimental determination of the surface coverage of oxygen and chlorine species using temporal analysis of products and prompt gamma activation analysis during HCl oxidation to Cl_2 on a RuO_2 catalyst. It is also substantiated by theory. We find that compensation phenomena appear when the effect on the apparent activation energy caused by changes in surface coverage is balanced out by the entropic configuration contributions of the surface. This result sets a new paradigm in understanding the interplay of compensation effects with the kinetics of heterogeneously catalysed processes.

Heterogeneous catalysis, a technology that selectively increases the rate of a desired chemical reaction[1], has become an invisible presence in our lives in the many chemical processes that utilize such catalysts. The large majority of surface reactions are temperature-dependent and obey the Arrhenius dependence; in other words, the rate (coefficient) is an exponential function of temperature. One peculiar observation is that for systems with varying activation energy, the activation energy E_{App} and pre-exponential factor A_{App} (parameters derived from Arrhenius analysis) can be interrelated. This 'compensation' phenomenon, also known as the Constable–Cremer relation, is a linear correlation between E_{App} and A_{App} such that[2–5]

$$\ln A_{App} = m\,E_{App} + c \qquad (1)$$

where m and c are constants.

Compensation phenomena may occur when the nature of the catalyst is systematically modified, the reactant is changed (within a family of related compounds) or when the pressures of the reactants and/or products are modified. The effect of a change in pressure is demonstrated with an experimental investigation of the Constable–Cremer relation for the Deacon reaction (gas-phase HCl oxidation; $4HCl + O_2 \leftrightarrow 2Cl_2 + 2H_2O$) in Fig. 1. This reaction, currently undertaken on an industrial scale over RuO_2-based catalysts[6–9], is an energy-efficient process used to manufacture chlorine from by-product HCl[10,11] and will serve as our example to study this phenomenon further.

A number of explanations for compensation have been proposed in the literature[5]. Classical views consider the Constable–Cremer relation to be a thermodynamic balance between the activation enthalpies and entropies when equation (1) is written as the Eyring version of transition state theory[12]. Bond *et al.*[5] reviewed the topic extensively and deduced that compensation can occur when the apparent Arrhenius parameters (that is, the rate and not the rate coefficients) are used to derive the Arrhenius parameters. As the rate is usually a complex function of the rate coefficient and surface coverage term(s), this implies that coverage is a crucial ingredient of the phenomenon. It has been postulated, however, without direct evidence, that compensation might be related to the temperature dependence of surface coverage.

Pioneering theoretical support for the key role of coverage was published by Bligaard *et al.*[13] on the basis of density functional theory simulations and microkinetics. Compensation was analysed from changes in the binding energy of surface intermediates, which induce a switch in the kinetic regime. It was shown that the stability of surface species modulates the coverage of free sites, which in turn affects both the activation energies and the pre-exponential terms. To obtain the Constable–Cremer relationship, the presence of a linear dependence between the activation energy and the enthalpy change of the critical reaction step (Brønsted–Evans–Polanyi relationships, BEP) was invoked. Later, microkinetic studies extended Constable–Cremer relationships to other model systems[14]. Monte Carlo simulations for adsorption also identified coverage terms as being responsible for compensation in adsorption[15].

All the investigations reported above are based on theoretical simulations on model systems and, because of the difficulties in quantifying the surface coverage of the reactants under reaction conditions, to date, no direct experiments have substantiated these theoretical insights. Here, we use state of-the-art experiments and calculations to show that a catalyst under different reaction conditions can yield the same activity, provided that the coverage terms of critical species are equal, and, at the same time, we show that a variation of

[1]Fritz-Haber Institute of the Max Planck Society, Berlin, D-14195, Germany, [2]Centre for Energy Research, Hungarian Academy of Sciences, Budapest, H-1525, Hungary, [3]Institute of Chemical Research of Catalonia (ICIQ), Av. Països Catalans 16, 43007 Tarragona, Spain, [4]Department of Chemistry, Technical University of Berlin, Berlin, D-10623, Germany, [5]Institute for Chemical and Bioengineering, Department of Chemistry and Applied Biosciences, ETH Zurich, Wolfgang-Pauli-Strasse 10, CH-8093 Zurich, Switzerland. *e-mail: teschner@fhi-berlin.mpg.de; nlopez@iciq.es

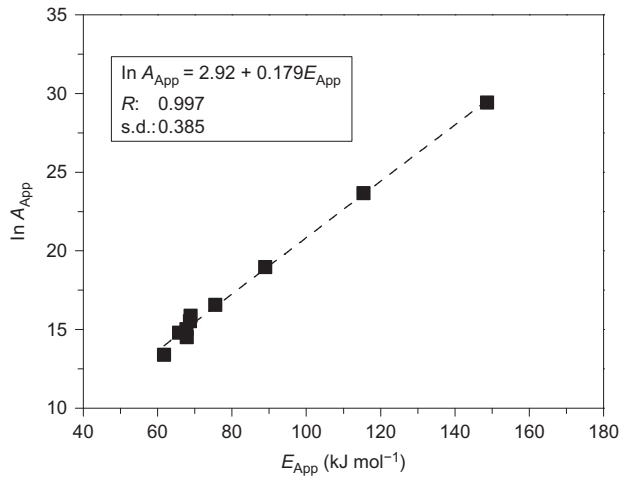

Figure 1 | Constable–Cremer relation for HCl oxidation over RuO_2/SnO_2-Al_2O_3. The Arrhenius parameters determined at different feed (O_2/HCl/N_2/Cl_2/H_2O) compositions correlate with one another and fulfil the Constable–Cremer relationship. Estimated isokinetic T is 671 K. RuO_2 is the active phase, SnO_2 is the carrier, and Al_2O_3 is used as a stabilizing agent and as the binder to prepare the technical catalyst (for details see ref. 11). Details of the individual Arrhenius experiments and parameters, and their standard errors, are given in Supplementary Fig. S1 and Table S6.

the reaction conditions gives rise to a Constable–Cremer relation. We link these two observations by introducing the term 'surface configurational entropy' to give a microscopic understanding of why coverage variations imply simultaneous changes in the activation enthalpies and entropies. We suggest that most compensation effects reported in heterogeneous catalysis can be derived on this basis.

Results and discussion

Model reaction. Surface reactions involve several elementary steps, and their kinetics may be understood by the use of reaction schemes. Many reactions, including but not limited to hydrogenations and oxidations, follow a general scheme with dissociative adsorption of H_2 or O_2. For the particular case of a reaction with stoichiometry, $1/2A_2 + B \leftrightarrow AB$, the Langmuir–Hinshelwood–Hougen–Watson mechanism can be written

$$1/2(A_2 + 2^* \leftrightarrow A_2^{**}) \quad \text{(R1)}$$

$$1/2(A_2^{**} \leftrightarrow 2A^*) \quad \text{(R2)}$$

$$B + ^* \leftrightarrow B^* \quad \text{(R3)}$$

$$A^* + B^* \leftrightarrow AB^* + ^* \quad \text{(R4)}$$

$$AB^* \leftrightarrow AB + ^* \quad \text{(R5)}$$

where the elementary reactions (R1)–(R5) are reversible microscopically and the number of surface sites is constant. Assuming that the dissociative adsorption of A_2 is the rate-determining step (alternatives are presented in Supplementary Table S1), the rate can be written as

$$r = \frac{1}{2}(K_1 k_2)^{1/2} \Theta^* \left(\frac{p_{A2}}{p^0}\right)^{1/2} (1-\beta) \quad (2)$$

where K_1 and k_2 are the thermodynamic constant and kinetic rate coefficient for A_2 adsorption and dissociation, respectively, p_i represents the partial pressure of A_2, B or AB, $p^0 = 1$ bar, Θ^* is the fraction of free sites and

$$\beta = \frac{1}{K_g}\frac{p_{AB}(p^0)^{1/2}}{p_{A_2}^{1/2} p_B}$$

is the approach to equilibrium for the overall reaction (where K_g is the overall thermodynamic constant).

Common practice indicates that for reactions to be industrially appealing they should be driven near or not too far from the maximum given by the Sabatier principle, which corresponds to the area of optimum binding energy of the critical reactant species[16]. Therefore, to reach efficiency, it is desirable that catalytic surfaces are highly populated under operating conditions, implying that the quantity of empty sites Θ^* is low (to improve the probability of surface reactions), as suggested from kinetic Monte Carlo simulations[17]. The configurational entropy associated with empty sites on the surface can be expressed as the logarithm of the binomial coefficient of the empty N^* and total N lattice positions $S = R\ln(N!/N^*!(N-N^*)!)$,[18] or, equivalently, $S = -R\Theta^* \ln \Theta^*$, where R is the universal gas constant. The reduction of the configurational entropy associated with A_2 adsorption is given by $\Delta S_{conf} = R \ln \Theta^* + R$. This is clearly seen in Supplementary Movies S1,2, where the number of configurations W is larger for the surface with a lower occupancy. For details on the derivation of S and the number of microstates W, see Supplementary Section S5. Equation (2) can then be rewritten as

$$\begin{aligned} r &= \frac{1}{2}(K_1 k_2)^{1/2}\left(\frac{p_{A2}}{p^0}\right)^{1/2}(1-\beta)\exp\left(\ln\left[\Theta^*\right]\right) \\ &= \frac{1}{2}(K_1 k_2)^{1/2}\left(\frac{p_{A2}}{p^0}\right)^{1/2}(1-\beta)\exp\left[\Delta S_{conf}/R - 1\right] \end{aligned} \quad (3)$$

which demonstrates the appearance of the entropic contribution related to the smaller number of surface configurations as a result of adsorption of A_2. The rate can be further expressed in the Eyring form[12], that is, in terms of enthalpic and entropic contributions:

$$\begin{aligned} r &\propto A_{mol}\exp\left(-\frac{\Delta H^{\ddagger}}{RT}\right)\exp\left(\frac{\Delta S_{conf}}{R}\right) \\ &= \exp\left(\frac{\Delta S_t + \Delta S_{conf}}{R}\right)\exp\left(-\frac{\Delta H^{\ddagger}}{RT}\right) \end{aligned} \quad (4)$$

where the molecular prefactor $A_{mol} = \left(\nu/N_0 e^2 \left(2\pi m k_B T\right)^{1/2}\right)^{1/2}$ is usually referred to as the thermal entropy contribution, ΔS_t, and contains the loss of translational freedom of A_2, and ν is the attempt frequency for dissociation associated with reaction (R2) (vibrational entropy contributions of the transition and initial states). Bligaard *et al.*[13] found the molecular prefactors to be rather constant (with a maximum variation of 10%). $\Delta H^{\ddagger}$ is equivalent to the apparent activation energy through the expression $E_{App} = \Delta H^{\ddagger} + RT$ (ref. 19). Thus, we have identified a new form of entropy related to the available configurations of active sites.

Going back to the Constable–Cremer relation, the Arrhenius parameters can be derived[16] according to the equations

$$\begin{aligned} E_{App} \equiv RT^2\frac{d\ln r}{dT} &= \frac{1}{2}\left(\Delta H_1 + E_{a,2}\right) - \Delta H_1 \Theta_{A2} \\ &+ \left(\Delta H_3 + \Delta H_4 + \Delta H_5\right)\Theta_A - \Delta H_3 \Theta_B \\ &+ \Delta H_5 \Theta_{AB} + \frac{\beta}{1-\beta}\Delta H_g \end{aligned} \quad (5)$$

and

$$\ln A_{App} \equiv \ln(r) + \frac{E_{App}}{RT} = \ln\left(\frac{1}{2}(K_1 k_2)^{1/2} p_{A2}^{1/2} \Theta^* (1-\beta)\right) + \frac{E_{App}}{RT} \quad (6)$$

The reader should note that equation (5) represents an analytical form of the phenomenological Temkin equation[20,21], where the apparent activation energy is reported to contain a part of the barrier from the rate-determining step with the addition of the adsorption enthalpies weighted by the coverage. Changes in the pressure of A_2, B and AB affect the coverage of all species on the surface, including the free sites. External pressures need to change by large amounts to affect coverage terms significantly, as A and B species compete for the same sites. Although the coverage term stored in the rate is smoothed by the logarithmic function, the contribution in E_{App} is linear (equations (5) and (6)). Thus, the coverage will contribute to E_{App} and ln A_{App} in a similar form, except if the rate is changed dramatically.

Accordingly, coverage variations can be responsible for modifications in both $\Delta H^{\ddagger}$ and ΔS_{conf}, so equation (4) adds to the interpretation of the coverage effects in compensation by indicating that coverage modifications imply configurational entropy contributions that impede dissociative adsorption of reactants on crowded catalytic surfaces.

Compensation phenomena have been described for other activation processes, such as diffusion, electrical conduction and dielectric relaxations[22]. In a few cases, entropy terms have been discussed as the missing link for compensation. Examples of these interpretations can be found for phase transitions[23], or in models as the 'multi-excitation entropy'[22] in which a higher barrier was thought to require a larger amount of molecular excitations. The surface configuration of the catalyst has a somewhat similar role in our description above.

HCl oxidation on RuO_2 catalysts: experimental assessment of coverage dependences. To date, coverage has been an elusive variable and highly challenging to quantify experimentally, so its key role in compensation phenomena has only been suggested theoretically[5,13–15]. However, coverage can be quantified by modern experimental methods. Our case study, HCl oxidation on RuO_2, was shown to fulfil the Constable–Cremer relationship (Fig. 1) and follows the mechanism (D1)–(D6) below (refs 24–29), for which the rate expression $r \approx r_2 = \frac{1}{2}k_{+2}^{1/2}\Theta_{O2} - \frac{1}{2}k_{-2}\Theta_O = \frac{1}{2}(K_1 k_2)^{1/2} p_{O2}^{1/2} \Theta^*(1-\beta)$ (see Supplementary Sections S5,6 for the derivation) has the same form as equation (2):

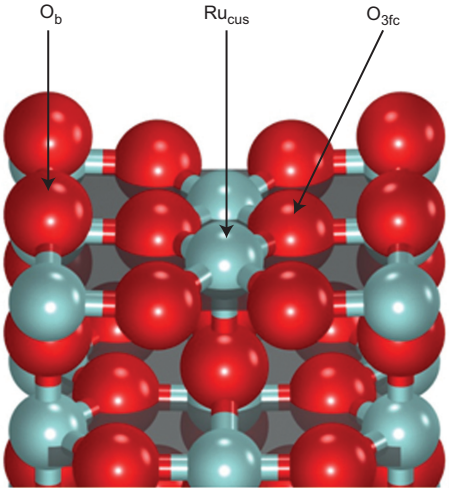

Figure 2 | Schematic representation of the RuO_2(110) surface. The surface contains three types of site: coordinatively unsaturated Ru sites (Ru_{cus}), two-fold coordinated (O_{3fc}) and bridging O (O_b).

$$O_2 + 2^* \leftrightarrow O_2^{**} \quad (D1)$$

$$O_2^{**} \leftrightarrow 2O^* \quad (D2)$$

$$HCl + O^* + ^* \leftrightarrow OH^* + Cl^* \quad (D3)$$

$$2Cl^* \leftrightarrow Cl_2 + 2^* \quad (D4)$$

$$2OH^* \leftrightarrow H_2O^* + O^* \quad (D5)$$

$$H_2O^* \leftrightarrow H_2O + ^* \quad (D6)$$

The surfaces of most RuO_2 facets show two types of site of interest (Fig. 2), coordinatively unsaturated Ru atoms (Ru_{cus}) and bridging O atoms (or bridging Cl under Deacon conditions)[29]. Evolution of H_2O or Cl_2 from bridge sites is not feasible (Supplementary Table S2), so it is the Ru_{cus} sites that play a dominant role in the reaction[25,26]. Chlorine recombination from Ru_{cus} positions is the most energy-demanding step[26,27,29], but at very high chlorine coverages, typical in the Deacon operation, the rate-determining step is catalyst re-oxidation[29]. Despite the somewhat more complex reaction scheme, the Deacon reaction fits well into the general model discussed above (compare (D1)–(D6) to (R1)–(R5)).

The temporal analysis of products (TAP) technique[30,31] enables evaluation of the oxygen coverage under reaction conditions while decoupling oxygen activation (D1)–(D2) and chlorine formation (D3)–(D6) steps. With this approach, the oxygen coverage can be modified quantitatively by varying the time delay between the O_2 and HCl pulses. To achieve this, experiments were conducted in the Knudsen diffusion regime as this ensures (i) a linear relationship between the area of the response and the amount of gas dosed and (ii) that the shape of the transient responses is independent of pulse size. By pulsing a mixture of Ar:O_2 (1:2) over a pre-chlorinated RuO_2 sample and over a blank reactor (loaded entirely with inert quartz particles), the amount of oxygen adsorbed on the catalyst as a function of time after pulse injection can be determined (for TAP details see Supplementary Section S2). The amount of oxygen adsorbed at time t is proportional to the difference in the areas below the transient responses of O_2 between zero and that time. The proportionality constant can be determined because the number of molecules per pulse is calibrated (11.8 nmol per pulse) and the total number of exposed Ru_{cus} sites on the sample that are able to adsorb oxygen is known (6.5×10^{18} sites/m^2)[28,29]. Figure 3a shows that the oxygen coverage increases until nearly 1 s, where it reaches a maximum, and then decreases continuously until it reaches zero at ~6 s. As expected, the values of coverage determined by TAP are noticeably lower than those determined under flow conditions (Fig. 4). This is intrinsic to the nature of the TAP experiment as a result of its operation in the sub-millibar pressure range and the fact that the number of O_2 molecules per pulse is 100 times lower than the number of exposed Ru_{cus} sites in the catalyst.

Pump–probe experiments were also carried out, consisting of pulsing Ar:O_2 (1:2, pump) then Kr:HCl (1:2, probe), separated by a time delay (Δt) in the range 1–8 s. The area of the chlorine response was monitored by mass spectrometry as a function of the time delay. Figure 3b unequivocally shows the linear dependence of chlorine production and oxygen coverage, in line with surface

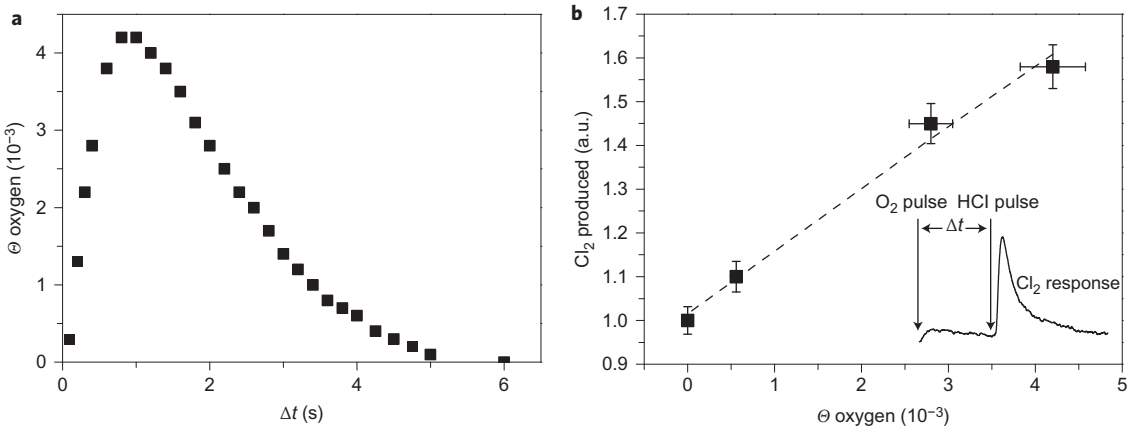

Figure 3 | TAP experiments identifying the role of surface oxygen. a, Oxygen coverage on RuO_2 as a function of time after pulse injection in the TAP reactor. **b**, Chlorine production as a function of oxygen coverage, as determined by the pump–probe experiment. Both experiments were conducted at 623 K. Inset (**b**): pump–probe experiment, in which chlorine production is monitored when pulsing O_2 (pump), followed by a probe pulse of HCl. Error bars are estimated from the accuracy in integrating the TAP responses and propagating the error throughout the whole calculation when averaging 10 pulse cycles.

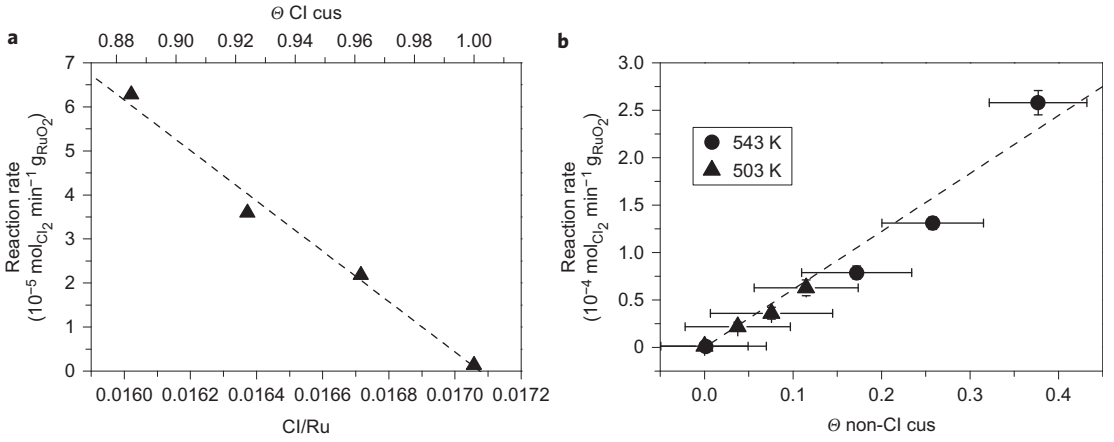

Figure 4 | *In situ* PGAA experiments evaluating the role of surface Cl. a,**b**, Dependence of the rate of Cl_2 production during the Deacon reaction on RuO_2 as a function of chlorine uptake and coverage of cus sites at 503 K (**a**) and of cus coverage by non-chlorine species at the two temperatures indicated (**b**). The reaction rate is first order to the coverage of cus sites not occupied by chlorine. The reaction was carried out at atmospheric pressure with feed composition $O_2/HCl/N_2$ varied between 0:1:4 and 4:1:0 at a total flow of 166.6 cm^3 STP min^{-1}. The coverage error bars include all deviation in calculating Cl/Ru ratios (including determination of the PGAA peak areas) and propagating the error through all calculation steps. Activity error bars are estimated from multiple iodometric titrations.

reoxidation (reactions (D1)–(D2)) being the critical step in the reaction. From back-extrapolation of chlorine production to null in Fig. 3b, it is estimated that the quantity of strongly adsorbed species not counted in Fig. 3a but giving rise to reactivity corresponds to a coverage of $\sim 7 \times 10^{-3}$.

To determine chlorine coverage as a function of the feed composition for which the Constable–Cremer relation was retrieved, we used cold neutrons to emit element-specific γ photons. By measuring these photons with a high-purity germanium detector, *in situ* prompt gamma activation analysis (PGAA) could be performed at ambient pressure[32,33]. Our DFT calculation indicates that the penetration of chlorine atoms into the lattice is energetically very demanding (>2 eV), so chlorination takes place exclusively in the outermost layer by replacing some O_b or by occupying empty Ru_{cus} positions, in agreement with ref. 24. This result enables the use of the intrinsically bulk-sensitive PGAA as a surface-sensitive technique for this particular problem. We first evaluated the maximum amount of chlorine uptake for Ru_{cus} and bridge sites individually (Supplementary Table S3), as well as for when both are occupied. The results indicate that each of these sites can be populated equally, and the maximal occupation of Ru_{cus} + bridge sites is the sum of the independently populated sites. The maximal occupation is defined as 100% coverage. Various steady-state Deacon feed conditions were then applied, and we found (Fig. 4a) that the reaction rate decreases linearly with increasing Cl uptake (*viz.* increasing chlorine coverage). Because the bridge sites hold chlorine species much more tightly (Supplementary Table S2), the derived variation in coverage is primary related to changes occurring at the Ru_{cus} sites. The modification of chlorine coverage can be expressed as coverage changes of oxygen-related species (plus free sites). This is shown in Fig. 4b, which includes data for two temperatures. Although the data are somewhat scattered, a linear (first-order) dependence on the non-chlorine coverage with a temperature-independent gradient can be obtained:

$$r = k\Theta(T, p_i) \tag{7}$$

The results in Fig. 4 indicate that the catalyst may exhibit the same activity under very different conditions, provided that the non-chlorine (oxygen) coverage is comparable. Under the range of reaction conditions used and in the temperature range of interest, we

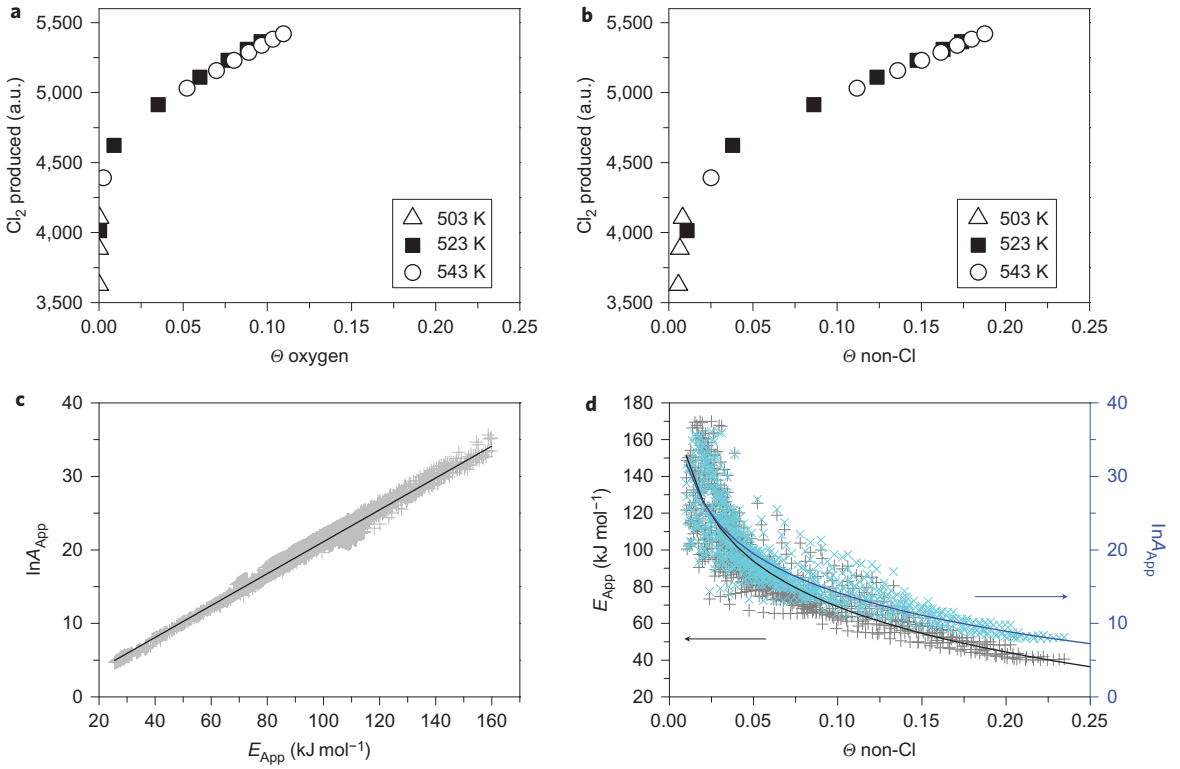

Figure 5 | DFT-based microkinetic modelling of the Deacon reaction over RuO_2(110) validates the effect of coverage in the compensation. a,**b**, Simulated DFT-MK Cl_2 production as a function of calculated oxygen coverage (**a**) and non-chlorine coverage (**b**), for different temperatures and O_2:HCl ratios p(HCl) = 0.2 bar; $p(O_2) = 0.05$–0.8 bar. **c**, Corresponding Constable–Cremer representation for mixtures of p(HCl) = 0.1–0.3 bar, $p(O_2) = 0.05$–0.8 bar, $p(Cl_2) =$ 0–0.1 bar and $p(H_2O) = 0$–0.1 bar, fitting ln $A_{App} = 0.22E_{App}$–0.53; $r = 0.99$. **d**, The origin of the Constable–Cremer relation is depicted as the dependence of both the apparent energy and prefactor on non-chlorine coverage. Solid lines correspond to fittings to $\ln\Theta(T,p_i)$, the logarithm of the non-Cl coverage.

can rule out surface structural or morphological changes in the catalyst because (i) the Arrhenius dependence (Supplementary Fig. S2) is very smooth and (ii) the RuO_2 gives a formal $p(O_2)$ dependence of 0.4 in the whole temperature range. In comparison, the rate of the model system (equation (2)) can also be linearized (Supplementary equations (S16)–(S19)), with an almost independent coefficient multiplied by a coverage-like term, as in equation (7).

Marrying experiments and theory through microkinetic modelling: the origin of compensation. To link the experimentally observed compensation, as well as the TAP and PGAA coverage determinations, to the rationale presented in the theoretical section, we performed microkinetic simulations (DFT–MK) on the Deacon reaction based on our previous DFT results[26,29]. These simulations aim to provide a consistent framework for the understanding of the dependencies found and the origin of the compensation. Multiple simulations at different temperatures and initial pressure ratios were run to obtain the rate, the coverage of relevant species, the Arrhenius dependencies and the Constable–Cremer relationship (Fig. 5). For instance, at the temperatures at which the PGAA experiments were performed with p(HCl):$p(O_2)$ ratios between 0.25 to 4, a linear relation between chlorine production and oxygen coverage (Fig. 5a) or non-chlorine coverage (Fig. 5b) was found for a large range of coverage values ($\Theta(T,p_i) =$ 0.05–0.20), following the trends in Figs 3b and 4b. Temperature and relative inlet pressure changes imply modification of the non-chlorine coverages, leading to a coverage term $\Theta(T,p_i)$ that contains the T and p contributions and a temperature-independent rate coefficient k in the form of equation (7). It is possible to trace back why points from different external variables produce the same rate (Table 1; see Supplementary Tables S4 and S5 for all constants). The $(K_1k_2)^{1/2}$ term shows a relatively weak temperature dependence (10%). Equations (2) and (7) imply that a change in the pressure (affecting β, p_{O2}) and temperature (changing β) is balanced by the number of free sites Θ^*. This is indeed what shows up in the simulation of conditions I ($T = 523$ K and p(HCl):$p(O_2) = 3$) and II ($T = 543$ K and p(HCl):$p(O_2) = 2$), for which a very similar value of non-chlorine species $\Theta(T,p_i)$ is obtained (for conditions I and II see Table 1).

For a larger set of conditions (about 4,000 simulations with different p(HCl):$p(O_2)$:$p(Cl_2)$:$p(H_2O)$ initial mixtures) the Arrhenius dependence has been obtained. The calculated apparent activation energy for the p(HCl):$p(O_2)$ reference mixture (1:1) is in good agreement with the experiment (70 kJ mol^{-1}, Supplementary Fig. S3). The apparent activation energy and prefactor pairs fulfil compensation through the Constable–Cremer relationship presented in Fig. 5c. The DFT–MK simulations provide the non-chlorine coverage for each of these simulations and thus it is possible to analyse the dependence of E_{App} and A_{App} on this parameter (Fig. 5d). Both apparent terms depend similarly on the logarithm

Table 1 | DFT analysis of the different contributions to the reaction rate.

	p_{o2} (bar)	T (K)	$(K_1\,k_2)^{1/2}$	Θ	$(r_{II}/r_I)_{DFT\text{-}MK}$	(r_{II}/r_I)
I	0.6	523.15	4.66	0.148	1.00	1.00
II	0.4	543.15	4.26	0.150	1.00	0.99

Simulated conditions: (I) p(HCl):$p(O_2) = 3$, $T = 523$ K; (II) p(HCl):$p(O_2) = 2$, $T = 543$ K. DFT calculated oxygen adsorption constant K_1 and kinetic coefficient for dissociation k_2. Non-chlorine coverage with respect to the maximum at a given temperature, $\Theta = \Theta_{Cl}^{max}$-$\Theta_{Cl}$, as obtained from the DFT-MK simulations. Also shown are the relative rates for points I and II $(r_{II}/r_I)_{DFT\text{-}MK}$ as obtained from the DFT-MK simulations, and by the direct product of constants $(K_1\,k_2)^{1/2}$ and the non-chlorine coverage on the surface, denoted (r_{II}/r_I).

of the coverage term. The reason for the significance of ln A_{App} becomes clear from equation (4) as it corresponds to the configurational entropy, which is a measure of $\ln\Theta(T,p_i)$. As for E_{App}, the contribution from the coverage terms expressed in equation (5) can be rewritten in terms of $\ln\Theta(T,p_i)$ and this is the leading term in the expansion. Note that the higher-order terms corresponding to the MacLaurin expansion of the natural logarithm of the coverage in equation (5) are almost constant (Supplementary equations (20)–(26)). Thus, the same coverage contribution that reduces the apparent activation energy (improving activity) results in a reduction of the pre-exponential factor by a similar amount (thus hindering activity). As a consequence, the observed rate is ultimately much less dependent on the coverage than any of the apparent terms, because they cancel out to a significant extent. In summary, on a Cl-crowded RuO_2 surface, oxygen needs to undergo many activation attempts in order to dissociate, increasing the effective activation energy, but this contribution is balanced by variation in the surface configurational entropy.

Conclusions

Coverage terms give rise to compensation between the apparent parameters of the Arrhenius equation in balancing out the activity by simultaneously affecting the activation energy and the prefactor. We present the first accurate experimental *in situ* quantification of surface coverage for a reaction that follows Arrhenius dependence and fulfils the Constable–Cremer relationship, showing that concurrent variations in coverage occur. We have related the rate-limiting coverage contributions to the configurational entropy term of active surface sites, thus providing an entropy–enthalpy correlation. In heterogeneous catalysis, under the pressure conditions where the correspondence between the configurational entropy and the coverage term holds (that is, rather crowded active sites), the Constable–Cremer relationship is followed naturally and the reaction is iso-kinetic for systems that exhibit similar effective coverages. This formulation derived for reaction feed variation can be extended to compensation observed with different catalysts or related reactants. When the energetics of the active site varies or the heat of adsorption of reactants changes, this will give rise to coverage modulation of the rate-limiting species, as described above, triggering compensation. The present interpretation improves the understanding of compensation effects in heterogeneous catalysis.

Methods

An experimental Cremer–Constable relation for the Deacon reaction was derived in a flow reactor from Arrhenius experiments in the temperature range 523–644 K over a RuO_2/SnO_2-Al_2O_3 catalyst, by varying the feed (p(HCl):$p(O_2)$:$p(N_2)$:$p(Cl_2)$:$p(H_2O)$) composition. Owing to the correlation of surface coverage and Arrhenius parameters described in the text, the derived Arrhenius parameters from the flow reactor experiments are necessarily integral values integrated over the catalyst bed length.

A polycrystalline RuO_2 sample (Aldrich 99.9% calcined at 773 K) with 10 $m^2\,g^{-1}$ Brunauer Emmett Teller surface area was used in the TAP and PGAA experiments to determine surface coverages *in situ*.

A TAP-2 reactor was used to study the Θ_O effect in HCl oxidation at 623 K. Pulses in the 10 nmol range allowed response shapes to be obtained that were independent of pulse size, indicating that mass transport is controlled by Knudsen diffusion. Θ_O during oxygen pulse evolution was quantified by a novel method based on the difference between the area-normalized responses in the presence and absence of adsorption. In the latter case, the catalyst was replaced by non-porous quartz particles. This enabled the measurement of Θ_O during pump–probe experiments when HCl was pulsed after O_2.

In situ PGAA was performed at the cold neutron beam of the Budapest Neutron Centre (BNC) (refs 32,33). RuO_2 (0.5 g) was loaded into a quartz reactor, and the Cl/Ru elemental ratio (surface Cl/total Ru) was measured under various feed compositions (pure Cl_2 or HCl, and Deacon mixtures) at different temperatures.

The revised Perdew-Burke-Ernzerhof (RPBE) functional[34] applied to slabs containing three layers of RuO_2(110) was calculated for the Deacon reaction with the Vienna ab initio Simulation Package (VASP) code. Projector augmented wave (PAW) pseudo-potentials for the inner electrons[35] were used, as well as a 400 eV cutoff energy for plane waves and $4 \times 4 \times 1$ k-point meshes[36]. Microkinetic modelling was performed by numerically solving the differential algebraic equations, and the kinetic constants were derived from DFT and statistical mechanics[14]. Initial mixtures were used that contained p(HCl) = 0.1–0.3 bar, $p(O_2)$ = 0.05–0.8 bar, $p(Cl_2)$ = 0–0.1 bar and $p(H_2O)$ = 0–0.1 bar ratios and temperatures in the T = 503–623 K.

Full methods are available in Supplementary Sections S1 to S4.

Received 28 March 2012; accepted 20 June 2012; published online 29 July 2012

References

1. Ertl, G., Knötzinger, H., Schüth, F. & Weitkamp J. (eds) *Handbook of Heterogeneous Catalysis* (Wiley-VCH, 2008).
2. Constable, F. H. The mechanism of catalytic decomposition. *Proc. R. Soc. Lond. A* **108,** 355–378 (1925).
3. Cremer, E. The compensation effect in heterogeneous catalysis. *Adv. Catal.* **7,** 75–91 (1955).
4. Wilson, M. C. & Galwey, A. K. Compensation effect in heterogeneous catalytic reactions including hydrocarbon formation on clays. *Nature* **243,** 402–404 (1973).
5. Bond, G. C., Keane, M. A., Kral, H. & Lercher, J. A. Compensation phenomena in heterogeneous catalysis: general principles and a possible explanation. *Catal. Rev. Sci. Eng.* **42,** 323–383 (2000).
6. Hibi, T., Nishida, H. & Abekawa, H. Process for producing chlorine. US patent 5,871,707 (1999).
7. Hibi, T. *et al.* Process for producing chlorine. European patent EP936184 (1999).
8. Wolf, A., Mleczko, L., Schlüter, O. F. & Schubert, S. Method for producing chlorine by gas phase oxidation. European patent EP2026905 (2006).
9. Wolf, A., Mleczko, L., Schubert, S. & Schlüter, O. F. Method for producing chlorine by gas phase oxidation. European patent EP2027063 (2006).
10. Seki, K. Development of RuO_2/rutile-TiO_2 catalyst for industrial HCl oxidation process. *Catal. Surv. Asia* **14,** 168–175 (2010).
11. Mondelli, C., Amrute, A. P., Schmidt, T. & Pérez-Ramírez, J. Shaped RuO_2/SnO_2-Al_2O_3 catalyst for large-scale stable Cl_2 production by HCl oxidation. *ChemCatChem.* **3,** 657–660 (2011).
12. Liu, L. & Guo, Q. X. Isokinetic relationship, isoequilibrium relationship, and enthalpy–entropy compensation. *Chem. Rev.* **101,** 673–695 (2001).
13. Bligaard, T. *et al.* On the compensation effect in heterogeneous catalysis. *J. Phys. Chem. B* **107,** 9325–9331 (2003).
14. Lynggaard, H., Andreasen, A., Stegelmann, C. & Soltze, P. Analysis of simple kinetic models in heterogeneous catalysis. *Prog. Surf. Sci.* **77,** 71–137 (2004).
15. Kang, H. C., Jachimowski, T. A. & Weinberg, W. H. Role of local configurations in a Langmuir–Hinshelwood surface reaction: kinetics and compensation. *J. Chem. Phys.* **93,** 1418–1429 (1990).
16. Chorkendorff, I. & Niemansverdriet, J. W. in *Concepts of Modern Catalysis and Kinetics* Ch. 2 (Wiley-VCH, 2003).
17. Temel, B., Meskine, H., Reuter, K., Scheffler, M. & Metiu, H. Does phenomenological kinetics provide an adequate description of heterogeneous catalytic reactions. *J. Chem. Phys.* **126,** 204711 (2007).
18. Atkins, P. & de Paula, J. *Atkins' Physical Chemistry* 8th edn (Oxford Univ. Press, New York, 2006).
19. Laidler, K. J. *Chemical Kinetics* 3rd edn (Prentice Hall, 1987).
20. Bond, G. C. Rosa, F. C. & Short, E. L. Kinetics of hydrolysis of carbon tetrachloride by acidic solids. *Appl. Catal. A. Gen.* **329,** 46–57 (2007).
21. Temkin, M. Relation between the apparent and the true activation energy of heterogeneous reactions. *Acta Physicochim. URSS* **2,** 313–316 (1935).
22. Yelon, A., Movaghar, B. & Crandall, R. S. Multi-excitation entropy: its role in thermodynamics and kinetics. *Rep. Prog. Phys.* **69,** 1156–1194 (2006) and references therein.
23. Estrup, P. J., Greene, E. F., Cardillo, M. J. & Tully, J. C. Influence of surface phase transitions on desorption kinetics: the compensation effect. *J. Phys. Chem.* **90,** 4099–4104 (1986).
24. Crihan, D. *et al.* Stable Deacon process for HCl oxidation over RuO_2. *Angew. Chem. Int. Ed.* **47,** 2131–2134 (2008).
25. Zweidinger, S. *et al.* Reaction mechanism of the oxidation of HCl over RuO_2(110). *J. Phys Chem. C* **112,** 9966–9969 (2008).
26. López, N., Gómez-Segura, J., Marín, R. P. & Pérez-Ramírez, J. Mechanism of HCl oxidation (Deacon process) over RuO_2. *J. Catal.* **255,** 29–39 (2008).
27. Studt, F. *et al.* Volcano relation for the Deacon process over transition-metal oxides. *ChemCatChem* **2,** 98–102 (2010).
28. Hevia, M. A. G., Amrute, A. P., Schmidt, T. & Pérez-Ramírez, J. Transient mechanistic study of the gas-phase HCl oxidation to Cl_2 on bulk and supported RuO_2 catalysts. *J. Catal.* **276,** 141–151 (2010).
29. Teschner, D. *et al.* An integrated approach to Deacon chemistry on RuO_2-based catalysts. *J. Catal.* **285,** 273–284 (2012).
30. Pérez-Ramírez, J. & Kondratenko, E. V. Evolution, achievements, and perspectives of the TAP technique. *Catal. Today* **121,** 160–169 (2007).
31. Gleaves, J. T., Yablonsky, G., Zheng, X. L., Fushimi, R. & Mills, P. L. Temporal analysis of products (TAP)—recent advances in technology for kinetic analysis of multi-component catalysts. *J. Mol. Catal. A* **315,** 108–134 (2010).

32. Revay, Z. *et al. In situ* determination of hydrogen inside a catalytic reactor using prompt γ activation analysis. *Anal. Chem.* **80,** 6066–6071 (2008).
33. Teschner, D. *et al.* The roles of subsurface carbon and hydrogen in palladium-catalyzed alkyne hydrogenation. *Science* **320,** 86–89 (2008).
34. Hammer, B., Hansen, L. B. & Nørskov, J. K. Improved adsorption energetics within density-functional theory using revised Perdew–Burke–Ernzerhof functionals. *Phys. Rev. B* **59,** 7413–7421 (1999).
35. Kresse, G. & Joubert, D. From ultrasoft pseudopotentials to the projector augmented-wave method. *Phys. Rev. B* **59,** 1758–1775 (1999).
36. Monkhorst, H. J. & Pack, J. D. Special points for Brillouin-zone integration. *Phys. Rev. B* **13,** 5188–5192 (1976).

Acknowledgements

The authors acknowledge support from ETH Zurich, BMBF Project 033R018A, Bayer MaterialScience, the ICIQ Foundation, MICINN (CTQ2009-07753/BQU), BSC-RES, the EU FP7 NMI3 Access Programme, a NAP VENEUS grant (OMFB-00184/2006) and the cooperation project between the Fritz-Haber Institute and the former Institute of Isotopes founded by the MPG. K. Honkala is thanked for valuable suggestions.

Author contributions

H.S and R.S. carried out and evaluated catalytic experiments to derive the Constable–Cremer relation. M.G.H. and J.P.R. performed and evaluated the TAP measurements. G.N.L. and N.L. carried out DFT calculations, microkinetic simulations and model system analysis. D.T., R.F., A.K.G. and L.Sz. performed and evaluated PGAA measurements. R.S. provided valuable suggestions for interpreting the results. D.T., J.P.R. and N.L. contributed to writing the manuscript.

Additional information

The authors declare no competing financial interests. Supplementary information accompanies this paper at www.nature.com/naturechemistry. Reprints and permission information is available online at http://www.nature.com/reprints. Correspondence and requests for materials should be addressed to D.T. and N.L.